Available online at www.sciencedirect.com

Manufacturing Letters

Manufacturing Letters 41 (2024) 429–434

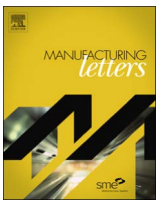

52nd SME North American Manufacturing Research Conference (NAMRC 52, 2024)

Milling infiltrated carbon-bonded carbon fiber: Geometric attributes, surface characteristics, and feasibility

Jake Dvorak[a,*], Dustin Gilmer[a], Ross Zameroski[a], Tony Schmitz[a,b]

[a]*Department of Mechanical, Aerospace, and Biomedical Engineering, University of Tennessee, Knoxville, TN 37996, USA*
[b]*Manufacturing Science Division, Oak Ridge National Laboratory, Oak Ridge, TN 37830, USA*

Abstract

This paper describes a manufacturing approach for carbon-bonded carbon fiber where cyanoacrylate and wax infiltration are used to improve the handling and machinability of preforms. Structured light optical coordinate metrology is used to acquire a stock model for computer-aided manufacturing and work coordinate system definition for machining. Non-infiltrated (neat) and infiltrated samples are machined using the same part program to compare results. Geometric attributes are measured with a touch trigger probe coordinate measuring machine and surface characteristics are measured with an optical 3D measuring system. Experimental results show superior geometric accuracy and surface roughness for the infiltrated samples over the neat sample.

Keywords: carbon-bonded carbon fiber; structured light scanning; infiltration; optical coordinate metrology;

1. Introduction

Carbon-bonded carbon fiber (CBCF) is a lightweight carbon/carbon composite first synthesized at Oak Ridge National Laboratory [1]. Due to its low thermal conductivity, high-temperature capability, and low density, it is commonly used in aerospace applications as thermal insulation [2]. The structure of CBCF results in high porosity of 70-90% [3]. CBCF is typically prepared via vacuum filtration, pressure filtration, dry formation or powder molding [2]. Due to the nature of these processes, they are limited to the creation of rectangular or cylindrical (non-complex) shapes. Improving the manufacturing process, properties, and performance of CBCF is an open research topic [4, 5, 6]. Few works in literature have explored milling of non-infiltrated CBCF and none have explored temporary infiltration of CBCF[7]. The purpose of this study is to test temporary infiltration and machining of CBCF to provide manufacturing capabilities for complex geometries.

Machining and handling of high porosity materials is challenging [8, 9]. Dust produced from the milling process can be a health hazard and cause direct wear and damage to a standard machine tool. The fragile nature of the preform requires slower cutting speeds and time-consuming fixturing. Milling of soft brittle materials results in microfracture damage and cracking on cut surfaces due to the lack of formation of an amorphous layer on cut surfaces [10]. This study seeks to alleviate these difficulties for milling CBCF using an infiltration process to temporarily densify the CBCF. Two forms of infiltration were selected. Infiltration of the CBCF preforms effectively increases the hardness of the preform, the preforms pressure on the tool during milling, resulting in a “protective” amorphous layer formation during milling. Cyanoacrylate was selected based on the authors successful previous research infiltrating a similar silicon carbide binder jet additively manufacturing preform [11]. This study used a similar methodology for coordinate system definition and stock model generation using structured light scanning. The second form of infiltration was paraffin wax which was selected for its common use in simi-

* Corresponding author. Tel.: +1-615-815-4007.
E-mail address: jaked@utk.edu (Jake Dvorak).

lar manufacturing applications, such as for infiltration prior to casting or infiltration prior to machining of metal foam [12, 13]. Exfiltration of CBCF parts is key to return the parts properties to their superior low density and low thermal conductivity after milling.

This study compares machining of neat, wax infiltrated, and cyanoacrylate infiltrated CBCF samples. A manufacturing sequence applied for similar low-density non-prismatic preforms is implemented, where a structured light scan of the preform is used to establish a coordinate system that can be identified in the machine tool and is used as the computer aided manufacturing (CAM) stock model for tool path generation [11]. Computer numerical control (CNC) end milling is used for all samples. The final geometry and surface characteristics of the samples are compared to establish feasibility of machining infiltrated CBCF. The intent is to improve the manufacturability of CBCF.

Nomenclature

ABS	acrylonitrile butadiene styrene
CAD	computer aided design
CAM	computer aided manufacturing
CBCF	carbon-bonded carbon fiber
CMM	coordinate measurement machine
CNC	computer numerical control
FFF	fused filament fabrication
WCS	work coordinate system

2. Methodology

Calcarb©CBCF rigid high-temperature insulation by Mersen was procured for this study. Three samples were cut from the starting block using a foam knife; see Figure 1a, where the sample sizes were approximately 30 mm by 30 mm by 25 mm. The first sample was designated as the "neat" sample and was not infiltrated. The second sample was infiltrated with 5 cP cyanoacrylate by pouring the cyanoacrylate on the top of the sample until it saturated the bottom of the sample. Excess cyanoacrylate was wiped off prior to drying. The third sample was infiltrated with paraffin wax inside an oven set to 75 °C. To facilitate the paraffin wax infiltration, a fused filament fabrication (FFF) acrylonitrile butadiene styrene (ABS) tower was designed and printed to hold wax above the CBCF sample; see Figure 1b. Aluminum stock was placed around the sample to maintain its position and facilitate removal. Wax pellets were added above the sample every few minutes until the wax was observed to saturate the base of the sample.

To enable handling and fixturing of the three samples without damage, the three samples were glued to a 25.4 mm by 25.4 mm by 152.4 mm section of aluminum bar stock. The bar stock and mounted samples was then clamped in a 101.6 mm wide machining vise; see Figure 2a. Scanning targets (1.5 mm) were attached to the vise and mounted samples. The entire setup was then scanned with a GOM ATOS Q structured light-based optical coordinate measurement system; see Figure 2b. This enabled the vise to serve as a fiducial for the machining work coordinate system (WCS) definition and the scan to be used as a stock model for the CAM tool path generation [11, 14]. Alignment of the three CAD sample models within the scan, the vise-based machining coordinate system, and CAM toolpaths are shown in Figure 3. The CAD alignments were made using a best-fit algorithm available in the GOM Inspect software. The alignment was completed in the XY plane for each sample 2 mm below the top surface. The machining coordinate system was defined by fitting three planes to three ground surfaces on the vise, again using GOM Inspect. CAM toolpaths consisted of two operations: 1) the top surfaces were faced; and 2) a 2D contour operation was completed around the sides. These operations targeted the first milling step towards manufacturing 12.45 mm tall, 25.4 mm diameter cylindrical pucks. A 7.94 mm diameter two flute titanium coated carbide bull nose endmill with a 0.2 mm corner radius by YG1 was used for all machining operations. Due to the high stiffness of the tool and low force level for material removal, the potential for unstable cutting (chatter) was low. A spindle speed of 7827 rpm, surface speed of 195.2 m/min, feed rate of 2082.8 mm/min, and feed per tooth of 0.133 mm were selected based on suggested parameters for similar hardness materials from the tool manufacturer. For the facing operation, a max stepover of 5.27 mm and step down of 0.5 mm were selected. For the 2D contour operation, a 1.27 mm max roughing stepdown was used with 0.76 mm of stock left radially for a finishing pass. The finishing 2D contour pass removed material 5 mm below the required bottom edge in a single pass for a total of 17 mm below the final top surface.

The vise with mounted samples was attached to the table in a Haas CM1 CNC milling machine; see Figure 4. The vise was aligned to the machine XY axes manually using a dial indicator. The three reference fiducial surfaces of the vise were probed using an on-machine touch probe (Renishaw OMP40) to identify the vise-based machining coordinate system. The CAM program was then uploaded to the machine and executed to machine the three samples. The operations were performed in the following sequence: faced cyanoacrylate infiltrated sample, faced wax infiltrated sample, faced neat sample, contoured cyanoacrylate infiltrated sample, contoured wax infiltrated sample, and contoured neat sample.

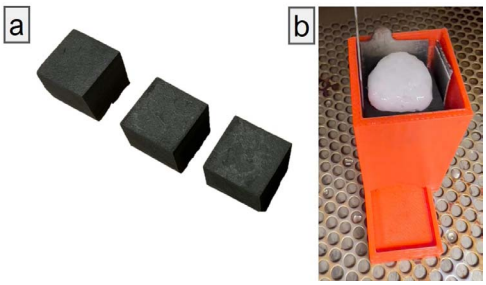

Figure 1. (a) Rough cut CBCF samples prepared for study; (b) wax sample infiltration using custom FFF printed tower in oven.

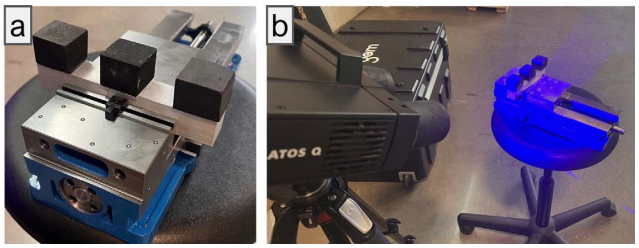

Figure 2. (a) Samples infiltrated and mounted to aluminum bar clamped in vise; (b) scanning of mounted samples for CAM and machining purposes.

3. Results

The three machined samples are shown in Figure 5. A noteworthy result was the clear distinction between observed chips from each sample; see Figure 6. The neat sample produced dust rather than chips, the cyanoacrylate-infiltrated sample produced a combination of dust and chips, and the wax-infiltrated sample produced chips similar typical machining results for ductile metals. Note that the large chips in the neat sample image were produced by another sample.

The diameter of each sample was measured using a ZEISS Duramax coordinate measuring machine (CMM). Two circular traces were completed on each sample that were located 4 mm and 8 mm below the top surface. Based on the mean diameter of 25.4 mm, the CMM results showed that the neat sample was -67 μm from nominal, the cyanoacrylate-infiltrated sample -34 μm from nominal, and the wax-infiltrated sample -33 μm from nominal. Therefore, both infiltrated samples provided a smaller diameter error.

Microscope images of each sample's top surface were completed using a Mitituyo Quickscope QS-L digital microscope; see Figure 7. Fewer gaps (dark areas) in the wax-infiltrated sample image indicate superior machining of the top surface as well as superior infiltration over the cyanoacrylate sample. The top surface was further investigated using an Alicona InfiniteFocusSL confocal microscope. A surface deviation map for all samples is shown in Figure 8. This result shows a uniform distribution of deviations in the neat sample. The cyanoacrylate-infiltrated sample shows the widest range of deviation. The wax-infiltrated sample shows the closest to nominal result with greater deviation in the center of the sample, suggesting that the infiltration was less successful at this location. This was likely due to the lack of a tight seal around the sides of the sample during infiltration, allowing wax to prioritize flowing along the sides of the sample. To analyze surface finish, five digital line traces were completed using the Alicona data; these traces conformed to ISO 4287 and 4288. The results are shown in Figure 9. The wax-infiltrated sample provided the lowest average roughness with an Ra of approximately 2 μm to 3 μm.

4. Conclusions

Based on the presented work and results, the following conclusions are made:

- Infiltration of CBCF with cyanoacrylate or paraffin wax improves its machinability by creating chips, rather than dust, during material removal similar to ductile metal machining.
- Infiltration of CBCF with cyanoacrylate or paraffin wax improves its machinability by densifying the workpiece and reducing the risk of damage during handling.
- Machined wax and cyanoacrylate-infiltrated CBCF samples exhibited more accurate geometry (diameter) compared to a neat CBCF sample.
- Wax-infiltrated CBCF resulted in superior surface finish over a neat sample or cyanoacrylate-infiltrated sample.
- The vise, which serves as the workpiece clamping system, can provide reference points for defining and aligning the WCS within a machine tool. This is achieved by including both the clamping system and the part in the structured light scan. This enables the WCS to be defined independently from the part geometry.

Future work plans to expand on the conclusions and address some of the shortfalls of this work. Greater focus will be made on the resulting chips for the various samples through further imaging. Vacuum infiltration will be used to produce samples with uniformly distributed internal infiltration material. Hardness of materials to be machined and machining forces and vibrations will be quantified. Testing various geometries, measuring tool wear, modifying methods of infiltration, and producing multiples of each sample are all planned efforts for future work.

Acknowledgements

This manuscript has been authored by UT-Battelle, LLC, under contract DE-AC05-00OR22725 with the US Department of Energy (DOE). The US government retains, and the publisher, by accepting the article for publication, acknowledges that the US government retains, a nonexclusive, paid-up, irrevocable, worldwide license to publish or reproduce the published form of this manuscript, or allow others to do so, for US government purposes. DOE will provide public access to these results of federally sponsored research in accordance with the DOE Public Access Plan (http://energy.gov/downloads/doe-public-access-plan)

References

[1] J. Cook, F. Lambdin, P. Trent, Discontinuous carbon–carbon composite fabrication., Tech. rep., Union Carbide Corp., Oak Ridge, Tenn. Y-12 Plant (1970).
[2] D. Yang, S. Dong, C. Hong, X. Zhang, Preparation, modification, and coating for carbon-bonded carbon fiber composites: a review, Ceramics International 48 (11) (2022) 14935–14958.
[3] C. Liu, J. Han, X. Zhang, C. Hong, S. Du, Lightweight carbon-bonded carbon fiber composites prepared by pressure filtration technique, Carbon 59 (2013) 551–554.
[4] Y. Zhang, Z. Lu, Z. Yang, D. Zhang, J. Shi, Z. Yuan, Q. Liu, Compression behaviors of carbon-bonded carbon fiber composites: Experimental and numerical investigations, Carbon 116 (2017) 398–408.

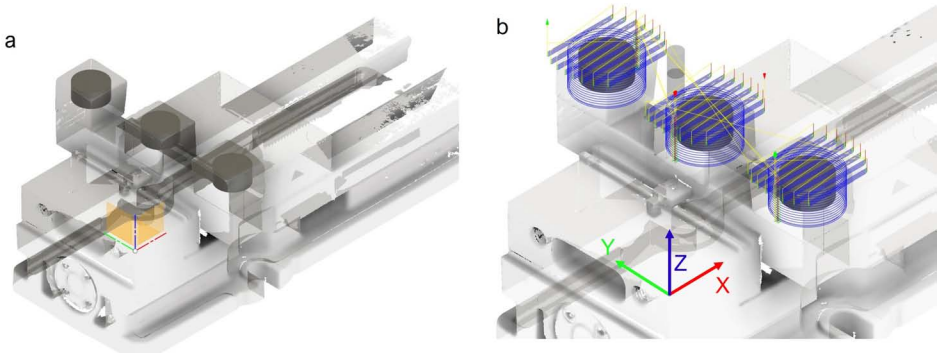

Figure 3. (a) Alignment of CAD within scan; (b) toolpaths generated based on alignment with WCS labeled.

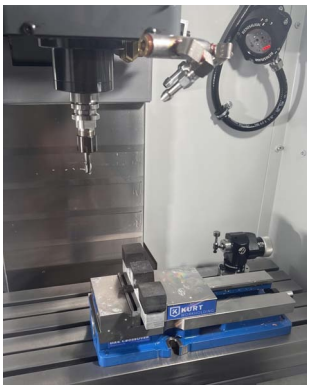

Figure 4. Preforms and vise mounted in milling machine.

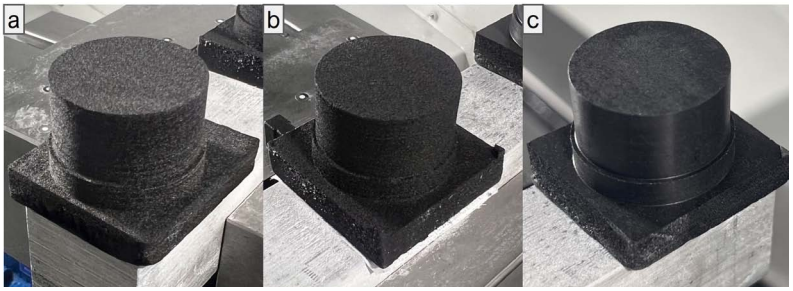

Figure 5. (a) Machined neat sample; (b) machined cyanoacrylate infiltrated sample; (c) machined wax infiltrated sample

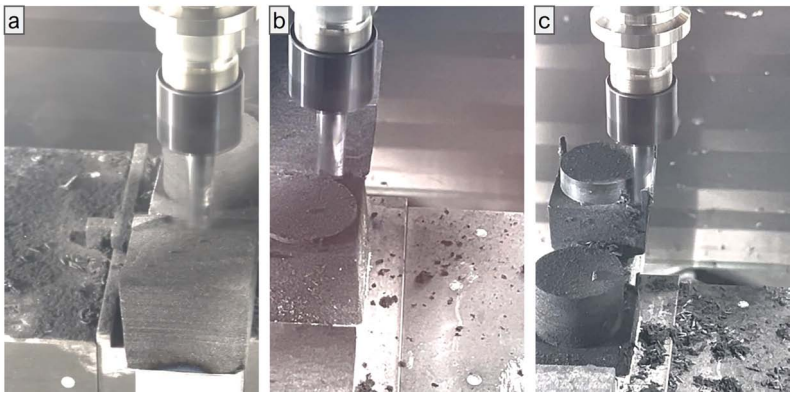

Figure 6. (a) Neat sample mid cut; (b) cyanoacrylate infiltrated sample mid cut; (c) wax infiltrated sample mid cut

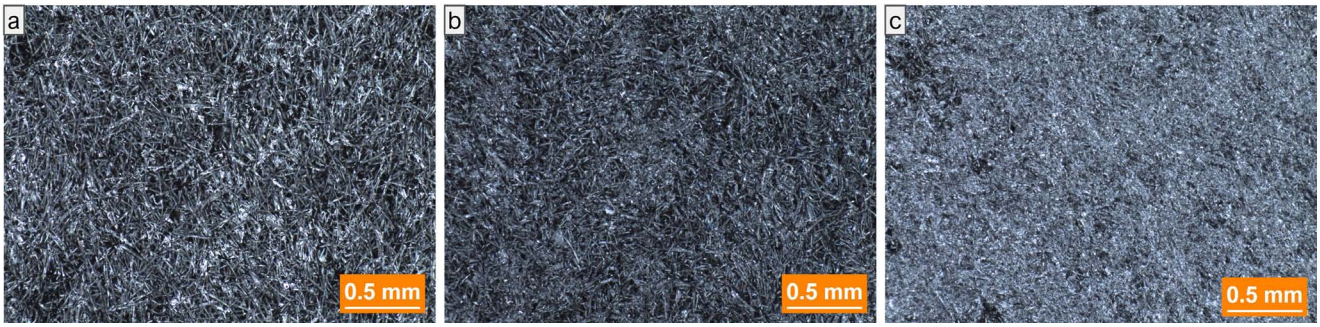

Figure 7. (a) Neat sample optical microscope image; (b) cyanoacrylate infiltrated sample optical microscope image; (c) wax infiltrated sample optical microscope image

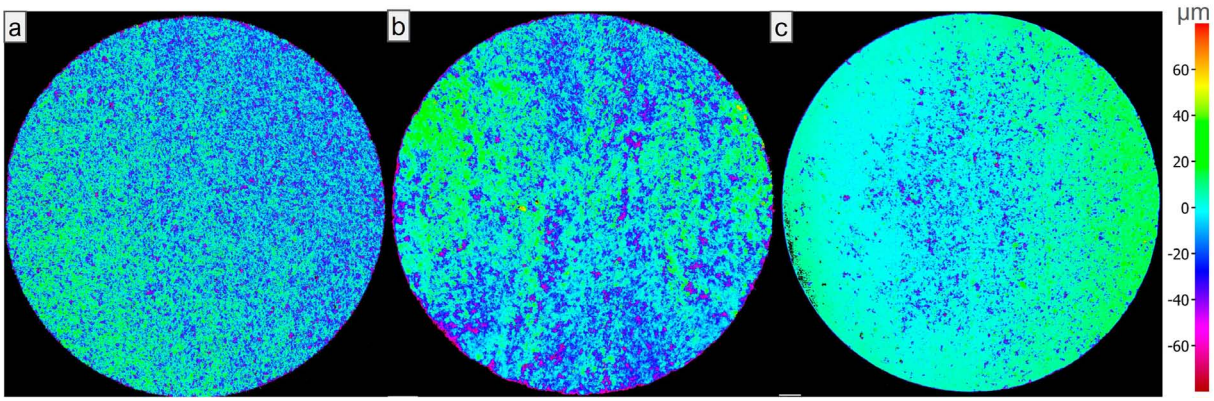

Figure 8. (a) Neat sample surface deviation map; (b) cyanoacrylate infiltrated surface deviation map; (c) wax infiltrated sample surface deviation map

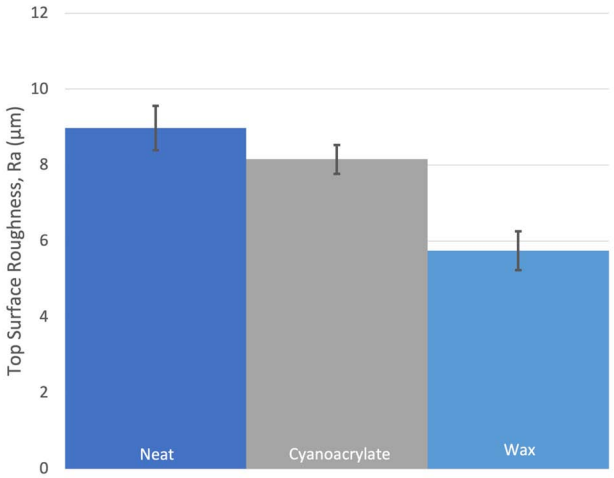

Figure 9. Surface roughness results.

[5] H. Cheng, C. Hong, X. Zhang, H. Xue, Lightweight carbon-bonded carbon fiber composites with quasi-layered and network structure, Materials & Design 86 (2015) 156–159.
[6] J. Li, J. Sha, J. Dai, Z. Lv, J. Shao, S. Wang, Z. Zhang, Fabrication and characterization of carbon-bonded carbon fiber composites with in-situ grown sic nanowires, Carbon 118 (2017) 148–155.
[7] G. Wei, J. Robbins, Development and characterization of carbon-bonded carbon fiber insulation for radioisotope space power systems, Tech. rep., Oak Ridge National Lab.(ORNL), Oak Ridge, TN (United States) (1985).
[8] S. Bhandarkar, T. Baumann, N. Alfonso, C. Thomas, K. Baker, A. Moore, C. Larson, D. Bennett, J. Sain, A. Nikroo, Fabrication of low-density foam liners in hohlraums for nif targets, Fusion Science and Technology 73 (2) (2018) 194–209.
[9] A. Laptev, M. Bram, H. Buchkremer, D. Stöver, Study of production route for titanium parts combining very high porosity and complex shape, Powder metallurgy 47 (1) (2004) 85–92.
[10] W. Huang, J. Yan, Effect of tool geometry on ultraprecision machining of soft-brittle materials: a comprehensive review, International Journal of Extreme Manufacturing 5 (1) (2023) 012003.
[11] J. Dvorak, D. Gilmer, R. Zameroski, A. Cornelius, T. Schmitz, Freeform

hybrid manufacturing: Binderjet, structured light scanning, confocal microscopy, and CNC machining, Journal of Manufacturing and Materials Processing 7 (2) (2023) 79.
[12] Castform™ ps material for sls systems, https://www.3axis.us/matetials/sls/CASTFORMHigh.pdf (2023).
[13] C. V. Hunt, A method to reduce smearing in the milling of metal foams, Iowa State University, 2009.
[14] J. Dvorak, A. Cornelius, G. Corson, R. Zameroski, L. Jacobs, J. Penney, T. Schmitz, A machining digital twin for hybrid manufacturing, Manufacturing Letters 33 (2022) 786–793.